

# Application of Skeletal Skinned Mesh Algorithm Based on 3D Virtual Human Model in Computer Animation Design

Zhongkai Zhan\*

Wuhan Vocational College of Software and Engineering, School of Arts and Media, Wuhan, 430205, China

**Abstract**—3D virtual character animation is the core technology of games, animation, and virtual reality. To improve its visual and realistic effects, the research focused on the skeleton skinned mesh algorithm. Firstly, a three-dimensional human body model was established based on motion capture data. Then, the skin vertex weight calculation and bone skin animation design were completed for the human body model. These experiments confirm that the designed weight calculation method has a smooth weight transition and good computational stability. The designed skinned mesh algorithm outperforms its skinned mesh algorithms in accuracy, recall, and area under curve values, with a maximum area under curve value of 0.927. Its smoothness and volume retention rate are both above 90.00%, and there is no obvious collapse phenomenon. Its other objective and subjective evaluation indicators are superior to the existing advanced skinned mesh algorithms processing, and the skin effect is realistic and smooth. Overall, this study contributes to the creation of 3D virtual character animation, enhances the visual realism of virtual creation, and provides key support for the animation performance of virtual characters.

**Keywords**—3D virtual human; skinned mesh algorithm; weight; character animation; dual quaternion; motion capture data

## I. INTRODUCTION

3D Virtual Character Animation (3DVCA) is a technology that uses computer to generate virtual character characters and complete animation drawing. As computer hardware, software, and graphics processing technology develop, 3DVCA plays an increasingly important role in people's work, learning, and daily entertainment life [1-2]. At present, 3DVCA has been widely applied in fields such as game development, film production, virtual reality, and augmented reality, and it belongs to a complex interdisciplinary field. Through 3DVCA, animation developers can create realistic and realistic virtual character images, enhancing user immersion and interactivity. [3-4]. However, creating highly realistic virtual human models requires rich anatomical knowledge and artistic skills, and the generation and control of virtual human actions need to consider multiple technical points such as human biomechanics, motion capture, and fusion. And bone skin binding technology still faces challenges in handling complex angle models, complex actions, and details. These unresolved technical challenges limit the application and development of 3DVCA [5]. How to build a more realistic simulation of human motion in 3D virtual character simulation has become a hot research topic. The advancement of dynamic simulation technology for 3D human models is of great significance for

the development of interdisciplinary fields such as entertainment, industry, and healthcare. And simulating human motion mainly involves the construction of dynamic models, precise motion behavior control systems, and the binding of bones and skin. In order to solve the technical difficulties in 3D virtual character simulation, the study chooses bone skin binding as the research core. Firstly, the motion capture data are analyzed to establish a 3D Virtual Human Model (3DVHM). On the basis of completing pose matching between the skin and bone models, a skin vertex weight calculation method is designed. Finally, the skeletal skin animation design is completed based on the dual quaternion mixed Skinned Mesh Algorithm (SMA). The innovation of the research is mainly reflected in the matching of skin and bone, as well as the study of skin deformation. On the one hand, the research innovatively designed a weight calculation method for skin vertices. Use a two-layer model to match and optimize poses, and calculate skin vertex weights in the area where bones affect the skin. On the other hand, research has optimized and improved the traditional linear hybrid skin Linear Blending Skinning (LBS) algorithm to avoid skin distortion and deformation, and to address the shortcomings of existing methods.

The research mainly includes four parts. Firstly, a review of the current research status of 3DVCA is completed, and summarized advanced research on 3D modeling. Then, the process of calculating skin vertex weights based on skin and bone pose matching was explained, and the steps of constructing an animation model based on the dual quaternion hybrid skin algorithm were explained; And the performance test results of the designed bone skin animation model are analyzed, and the skin effects were compared in application. Finally, the experimental results are summarized and summarized. This study is expected to contribute to the development of 3DVCA, providing a theoretical foundation and application technology for the research of computer graphics and computer animation.

## II. RELATED WORKS

3DVCA is currently a hot topic of concern in animation, film and television, and human-computer interaction. To further improve the modeling realism of virtual characters and models, scholars have conducted research on 3D modeling related technologies. The B-spline curve of a disk is an effective modeling tool based on control points, which can directly model regions or shapes with adjustable thickness.

However, the boundary curves of the shape described by the B-spline curve of the disk often exhibit self-intersection, which has a negative impact on the shape and texture of the model. Kruppa et al. designed an iterative algorithm that utilized the approximate circular skin method to handle the details of 3D model modeling. This method could generate smooth shape textures around sharp curved parts [6]. Although physical simulation can improve the detailed dynamic motion of animated characters, these are post-processing added after the overall animation modeling is completed. Wu et al. designed a new interactive framework based on position-based dynamic unified skin transformation and kinematic simulation. This framework had the advantages of controllable skin transformation and shape preservation, ensuring the efficiency, simplicity, and stability of model creation [7]. Implicit skinning in geometric interactive skinning methods is commonly used to solve skin self-collision and handle reasonable deformation at joints, requiring more user interaction to fully parameterize. Hachette et al. designed a specialized optimization framework for implicit skinning based on particle systems and dynamic shell meshes, and optimized the shape of the filled mesh to achieve reasonable skin deformation at joint rotations [8]. The same topology structure as the human body can produce the most realistic animation effects in digital clothing body animation, but its application limitations are strong. Peng et al. designed a graph convolutional network based on deep learning that could generate realistic clothing animations. This model was suitable for clothing types that did not match the body topology. Qualitative and quantitative experiments had verified that the model achieved state-of-the-art 3D clothing animation performance [9].

Mouhou et al. designed a real-time method for generating mesh deformation based on implicit skinning using spherical primitives, considering skin contact and muscle swelling simulation. This technique compensated for the shortcomings of linear hybrid skinning, allowing the model to handle network deformation reasonably while handling collisions and preserving mesh details [10]. The existing algorithms for reconstructing body surface models based on video sequences lack modeling of the internal structure of the human body. Zhao et al. created a four-dimensional animation process based on a personalized motion full anatomy digital model of videos. They estimated the internal structure of the human body using deformable human anatomy maps and simulated the movement deformation of soft tissues through smooth nonlinear transformations. These experiments confirmed that this method surpassed existing video-based body surface modeling methods [11]. The existing dynamic 3D modeling relies on data-driven learning and optimization, but has poor robustness in tracking different features in space and time. Moreover, the grid-based linear hybrid skin model has problems optimizing the network while maintaining a consistent mesh topology. Singla et al. proposed a new algorithm for reconstructing dynamic human body shapes using sparse contour information, and the robustness of this method was verified [12]. Neural networks are crucial for 3D reconstruction and new view synthesis of rigid scenes. Chen et al. designed a connection module based on neural fields, which utilized voxel-based corresponding search and

pre-computed linear hybrid skin functions. It could achieve precise correspondence between the normative space and the constituent space, effectively optimizing shape and skin weights [13]. Li D et al. designed a static skin model based on joint increment and skin weight increment to accurately predict dynamic fabric deformation. After testing in Unity game scenarios, the model achieved real-time prediction of fabric dynamics, and the network performed well in accurately capturing fine dynamic fabric deformation [14].

In summary, there have been many studies on 3D modeling, but there is still relatively little research on the improvement and optimization of bone-skin binding algorithms. Based on 3DVCA, this study conducts relevant research on the quality improvement and technical optimization of bone-skin binding algorithms.

### III. DESIGN OF SKELETAL SKINNED MESH ALGORITHM BASED ON 3D VIRTUAL HUMAN MODEL

To achieve more realistic and smooth character animation effects, research is conducted on bone SMA in 3DVCA, and methods for calculating skin vertex weights and dual quaternion mixed SMA are designed.

#### A. Calculation of Skin Vertex Weights Based on Skin and Bone Pose Matching

The modeling and detail processing of 3DVCA require a lot of time and human resources. In virtual character models, bone skin binding technology is responsible for connecting the character model with the bone system, ensuring that the skin can naturally follow the changes of the bones during animation [15]. However, bone skin binding technology still encounters issues such as occlusion, distortion, and skin vertex detachment when dealing with complex character models, complex actions, and details. Therefore, the study first calculates the weight of skin mesh vertices.

3DVHM includes skeletal structure, skin, muscle structure, and other details. Motion capture data are important resources for constructing and driving the motion of the 3DVHM [16]. They refer to real human motion data recorded through sensors or cameras, including joint positions, motion trajectories, and postures of the human body. Common motion capture data formats include ASF/AMC, BVH, C3D, etc. The study used ASF/AMC format to drive the 3DVHM. ASF contains skeleton information, defining the initial state of motion, while AMC is a motion data file. The separation of skeleton and motion information facilitates their matching [17]. Eq. (1) is the motion data frame in AMC format. In Eq. (1),  $f_i$  represents motion data.  $r_i^j$  represents the rotation information of the bone segment  $j$  in frame  $i$ .  $t_{i,x}^0, t_{i,y}^0, t_{i,z}^0$  represent the translation components of the root node in the world coordinate system.

$$\begin{cases} f_i = \langle t_i^0, r_i^0, r_i^1, r_i^2, \dots, r_i^n \rangle \\ t_i^0 = (t_{i,x}^0, t_{i,y}^0, t_{i,z}^0) \\ r_i^j = (t_{i,x}^j, t_{i,y}^j, t_{i,z}^j) \end{cases} \quad (1)$$

The study uses a skin-bone two-layer model to construct a human bone model, numbers and names the root nodes in the ASF file, and defines the hierarchical relationship between different joint points. Bones are formed between joint points, and the end joint points store the length and direction information of the bones. The root node and joint points contain 6 and 2 degrees of freedom information, respectively, to ultimately obtain a human skeleton with physical and activity characteristics. On this basis, the study uses the 3D modeling software 3D Max to complete the 3D human body modeling, and uses the Open GL function library to draw a polygonal mesh model to obtain modeling effect map.

To drive the human skin mesh model, it is necessary to establish a connection between the skin mesh and the joints or bones, that is, to calculate the weight of the influence of bones near the skin on the skin vertices. Maya software is used to establish a skin bone model that matches the skin model, and posture matching is performed with the motion bone model constructed from ASF files. The bone node information in the skin bone model is exported, and its joint node information is consistent with the definition of the bone model in the ASF file. The initial posture matching first calculates the bone length and completes the matching of limb length. Then, the angle information between different bones is corresponded one-to-one, and the joint direction information of the skin bone model is assigned to the moving bone model.

Usually, Maya software uses the nearest distance algorithm to calculate the range of action of bones on the skin. But it only considers the distance between bone and skin vertices, ignoring the hierarchical relationship of joints will increase the estimation error of the range of action. Therefore, the study extends a certain size of bone bounding boxes along the direction of the bone and perpendicular to the bone, and uses AABB bounding boxes to divide the bone model into different regions. Based on the bone bounding boxes, the impact of the bone on the skin is determined. Fig. 1 shows the skeleton bounding box.

The specific calculation of bounding boxes generally

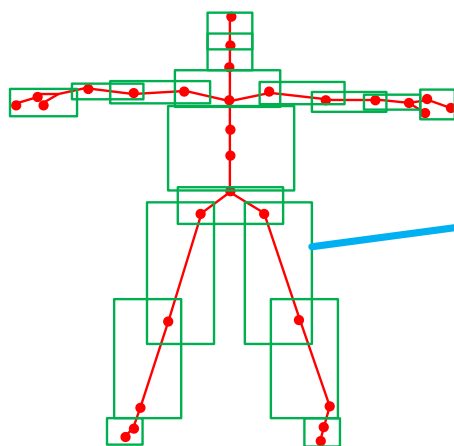


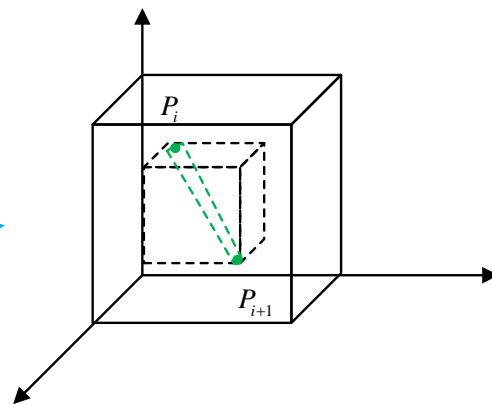
Fig. 1. Schematic diagram of the skeleton bounding box.

includes data pre-processing, determining expansion direction, and expanding bounding boxes. Firstly, based on the local coordinates of the joint points and bone information, the global coordinates of the joint points are obtained. The joint point coordinates of the bone are  $P_i$  and  $P_{i+1}$ , respectively. The projection lengths of bones on different coordinate axes are represented as  $x_{i+1} - x_i$ ,  $y_{i+1} - y_i$ , and  $z_{i+1} - z_i$ , respectively. The direction with the greatest change in length is approximately the bone's direction. The expansion coefficient of the bounding box is determined based on the human body structure. The bounding boxes of adjacent bones should intersect at a common joint point, and the expansion coefficient at the intersection is one-fifth of bone's length. The thickness of the bounding box at the bone cross-section is the thickness from the bone to the skin. However, considering the differences in bone and skin thickness in various parts of the human body, the cross-sectional expansion coefficient was set to one-third of the bone length. Fig. 2 shows the bounding box extension area.

The bone bounding box is defined as  $B_i$ . The criterion for determining whether the skin vertex  $v_i(x_v, y_v, z_v)$  is in the bounding box is represented by Eq. (2).

$$\begin{cases} x_{\min} - \frac{1}{3}length \leq x_v \leq x_{\max} + \frac{1}{3}length \\ y_{\min} - \frac{1}{3}length \leq y_v \leq y_{\max} + \frac{1}{3}length \\ z_{\min} - \frac{1}{3}length \leq z_v \leq z_{\max} + \frac{1}{3}length \end{cases} \quad (2)$$

Fig. 3 shows the calculation principle of skin vertices. When the skin vertex is a non-joint vertex, the weight size is related to the distance between the joint and the skin vertex, and the joint weight is calculated using the linear gradient method. When the skin vertex is a vertex at a joint, it will be affected by three joints.



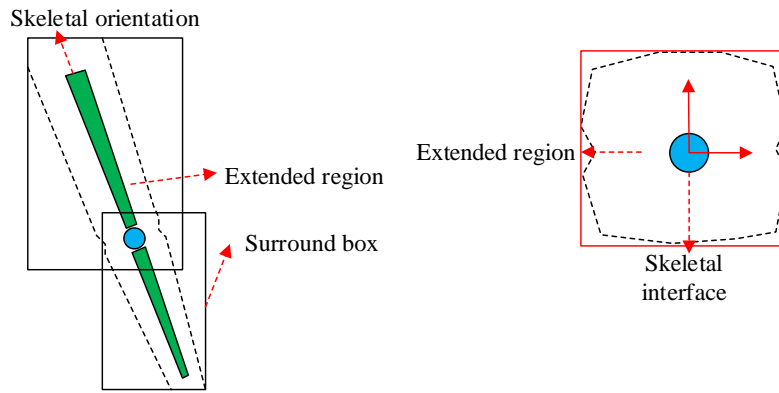


Fig. 2. Schematic diagram of the bounding box extension area.

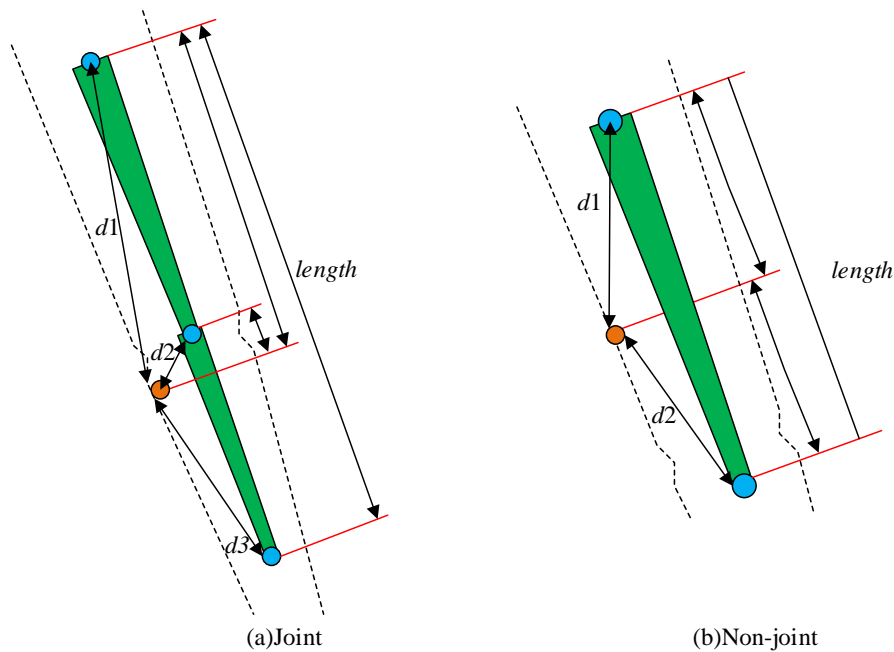


Fig. 3. Calculation principle of skin apex.

If the skin vertices are non-joint vertices, the weight calculation is represented by Eq. (3).  $w_a$  and  $w_b$  respectively represent the weights of the joint points at both ends of the skeleton within the bounding box.  $D_1$  and  $D_2$  respectively represent the projection of the distance from the skin vertex to the joint points at both ends in the bone direction.

$$\begin{cases} \frac{w_a}{w_b} = \frac{D_2}{D_1} \\ w_a = \frac{D_2}{D_1 + D_2} \\ w_b = \frac{D_1}{D_1 + D_2} \end{cases} \quad (3)$$

If the skin vertex is a vertex at the joint, the weight calculation is represented by Eq. (4).  $w_a, w_b, w_c$  are the joint weights.

$$\begin{cases} w_a : w_b : w_c = \frac{1}{D_1} : \frac{1}{D_2} : \frac{1}{D_3} \\ w_a = \frac{D_2 D_3}{D_1 D_2 + D_2 D_3 + D_1 D_3} \\ w_b = \frac{D_1 D_3}{D_1 D_2 + D_2 D_3 + D_1 D_3} \\ w_c = \frac{D_1 D_2}{D_1 D_2 + D_2 D_3 + D_1 D_3} \end{cases} \quad (4)$$

### B. Animation Model Design Based on Dual Quaternion Hybrid Skinned Mesh Algorithm

Skin deformation is the process of transforming the skin of one object onto another object, commonly used in applications such as character animation, model fusion, and deformation [18]. It is very important in 3DVCA and plays a crucial role in achieving realistic and smooth character animation effects. SMA is an important algorithm in skin deformation

technology. It associates the skeletal system of the 3D human model with the skin mesh, updates the position of the skin mesh vertices in the world coordinate system, and enables the character's skin to naturally follow the movement changes of the bones during animation [19]. The performance of SMA is related to the deformation and transformation of animated characters, determines the adjustment of model details and quality, and directly affects the efficiency and performance of rendering. The selection of SMA is very important.

Homogeneous coordinates and matrix forms are used to describe the coordinate changes in three-dimensional space. The homogeneous coordinate change is represented by Eq. (5).  $(x, y, z)$  is the original coordinate.  $(x', y', z')$  is a homogeneous coordinate.  $h$  means the scaling factor.

$$(x, y, z) \Rightarrow \begin{cases} x = x' / h \\ y = y' / h \\ z = z' / h \end{cases} \quad (5)$$

The skin vertex undergoes translation or rotation transformation, and the transformed skin vertex  $v'$  is represented by Eq. (6).  $\mathbf{M}$ ,  $\mathbf{T}$ , and  $\mathbf{R}$  are skin vertex change, translation transformation, and rotation transformation matrices, respectively. The rotation matrix can be decomposed into the rotational changes of a point around three coordinate axes.

$$\begin{cases} v' = \mathbf{M} \cdot v \\ \mathbf{M} = \mathbf{T} \cdot \mathbf{R} \end{cases} \quad (6)$$

The motion of the designed 3D virtual is based on the global coordinate system, and the basic position of the model is determined by the root nodes and joint points of the skeleton. The motion of the joint points is defined relative to the position of the parent node, and these two affect each other. So the base coordinate system and local coordinate system in Fig. 4 are introduced to describe this bone model. The base coordinate system refers to the coordinate system established with the sacral joint point as the origin in the initial pose of a three-dimensional virtual human. The local coordinate system is the rotational information defined relative to the global coordinate system.

The change in the coordinate line of any joint point is represented by Eq. (7).  $\varphi$ ,  $\alpha$ , and  $\beta$  are the angles at which a node rotates around  $z, x, y$  axes.  $G_i$  represents the rotation offset matrix of the related node relative to the parent node in the world coordinate system.

$$G_i = R_z^z(\varphi) \cdot R_x^x(\alpha) \cdot R_y^y(\beta) \cdot T_i \cdot [R_z^z(\varphi)]^{-1} \cdot [R_x^x(\alpha)]^{-1} \cdot [R_y^y(\beta)]^{-1} \quad (7)$$

The global change matrix  $M_i$  is represented by Eq. (8).  $f(i)$  is the parent node number of the joint point.  $F$  means a set of all node numbers.  $G_0$  represents the global affine transformation matrix of the root node,  $G_0 = R_0 \cdot T_0 \cdot R_0^{-1}$ .

$$M_i = G_0 \cdot \dots \cdot G_{f(i)} \cdot G_i = \prod_{k=0, k \in F}^i G_k \quad (8)$$

SMA uses transformation matrices to bind skin and bones, and the calculation of LBS is represented by Eq. (9).  $v'$  and  $v_0$  are the positions of skin vertices after and before the transformation, respectively.  $n$  represents the number of bones that affect the current skin.  $D_i$  means the global affine transformation matrix from the local coordinates of the skeleton to the global coordinates in the initial state of the model, and its calculation is similar to  $M_i$ .

$$v' = \sum_{i=1}^n w_i M_i D_i^{-1} v_0 \quad (9)$$

The transformation process from skin vertices in the global coordinate system to the local coordinate system in the initial state is the inverse transformation of Eq. (9). After transformation, AMC data are used for motion transformation to complete skin deformation. The deformation calculation is consistent with Eq. (8), and the values of the rotation offset matrix are analyzed and read based on AMC data. Fig. 5 shows the working mechanism of the entire LBS.

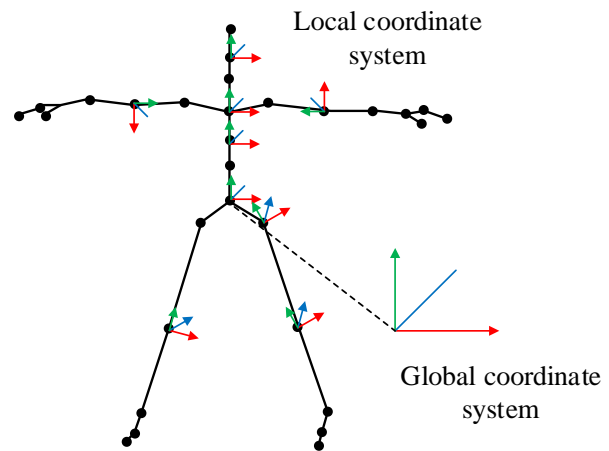


Fig. 4. Global coordinate system and local coordinate representation.

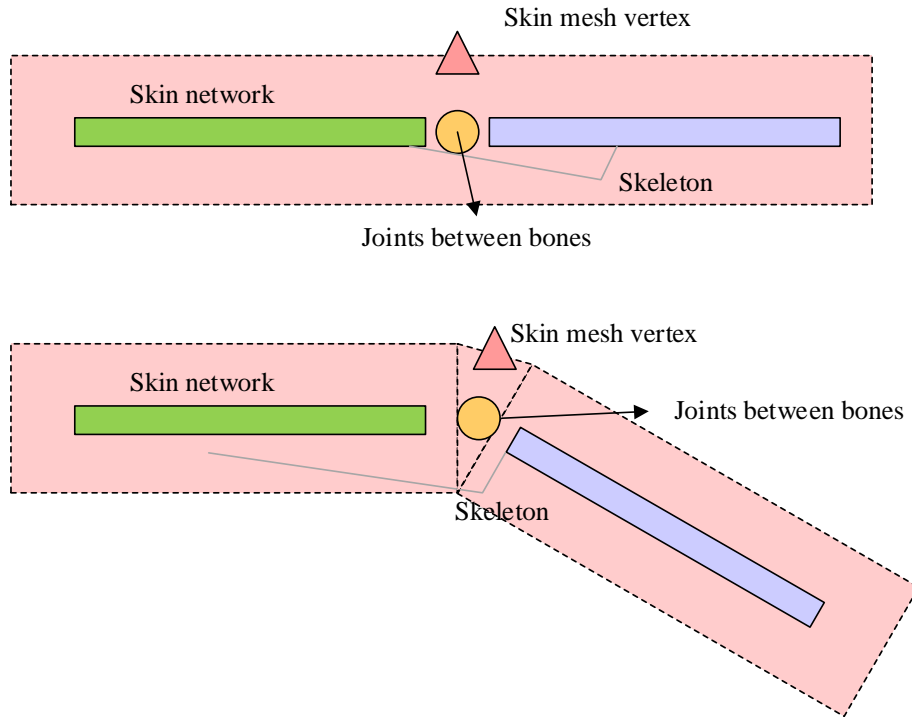


Fig. 5. Schematic diagram of skin deformation.

LBS is widely used in skin deformation calculation, but there are still significant application defects in LBS. LBS calculates bone influence weights through linear interpolation. When vertices are affected by multiple bones or overlap with multiple bones, it is easy to cause volume scaling or cross deformation problems [20]. Therefore, the study improves on the basis of LBS and designs a dual quaternion hybrid SMA using dual quaternions. The dual quaternion  $\mathcal{Q}$  consists of pairs of even numbers and quaternions, the two expressions for even numbers are given in Eq. (10). One way of expressing this can be understood as a quaternion in which all elements of the formula are pairs of even numbers, and the other expression can be understood as a quaternion in which all elements are pairs of even numbers.  $w, x, y, z$  are even numbers.  $q, q_\varepsilon$  are quaternions, representing the real and dual parts respectively, the real part contains the rotation information.  $\varepsilon$  means dual units.  $i, j, k$  are orthogonal unit vectors.

$$\begin{cases} \mathcal{Q} = w + i\mathcal{X} + j\mathcal{Y} + k\mathcal{Z} \\ \mathcal{Q} = q + \varepsilon q_\varepsilon \end{cases} \quad (10)$$

The unit dual quaternion of the three-dimensional space vector  $\vec{r} = (r_0, r_1, r_2)$  is represented by Eq. (11). When  $q_\varepsilon = 0$ ,  $\mathcal{Q}\mathcal{Q}^*$  means the rotational transformation of the rigid body.  $\mathcal{Q}^*$  and  $\overline{\mathcal{Q}}$  are conjugate and dual conjugate of dual quaternions, respectively.

$$\hat{r} = 1 + \varepsilon (r_0 i + r_1 j + r_2 k) \quad (11)$$

The unit dual quaternion of the translation transformation vector  $\vec{t} = (t_0, t_1, t_2)$  of a rigid body is represented by Eq. (12).  $\mathcal{Q}\mathcal{Q}^*$  is the translation transformation of a rigid body.

$$\hat{t} = 1 + \frac{\varepsilon}{2} (t_0 i + t_1 j + t_2 k) \quad (12)$$

The process of a rigid body rotating first and then translating in three-dimensional space is represented by Eq. (13), which means that the dual quaternion  $\hat{t}\hat{q}$  can achieve the process of rotating first and then translating.

$$\hat{t}(\hat{q}\hat{v}\hat{q}^*)\hat{t}^* = (\hat{t}\hat{q})\hat{v}(\hat{t}\hat{q})^* \quad (13)$$

The transformation matrix in LBS is converted into a dual quaternion, and the translation information in the matrix is defined as  $a = (a_{14}, a_{24}, a_{34})$ . The transformation between the translation matrix and the unit dual quaternion is represented by Eq. (14).

$$(a_{14}, a_{24}, a_{34}) = (t_0, t_1, t_2) \quad (14)$$

The coordinate of the skin vertex position  $p'$  after linear mixing of dual quaternions is represented by Eq. (15).  $P$  is the position coordinate of the current skin mesh vertex.  $w_i$  is

the weight. Eq. (15) represents the process of mixing and unitizing the global transformation matrix according to the weight values after transforming it into dyadic quaternions.

$$p' = \frac{\sum_{i=1}^n w_i q_i}{\left\| \sum_{i=1}^n w_i q_i \right\|} p \quad (15)$$

Through this change, LBS converts the linear transformation of the global transformation matrix  $E_i = M_i D_i^{-1}$  into linear mixing of dual quaternions. The mixing of dual quaternions was completed based on the weight size. The mixed dual quaternions are unitized and then transformed into a transformation matrix, which are multiplied by the coordinates of the skin vertices to update the skin vertices. Fig. 6 shows the workflow of the entire dual quaternion mixed SMA.

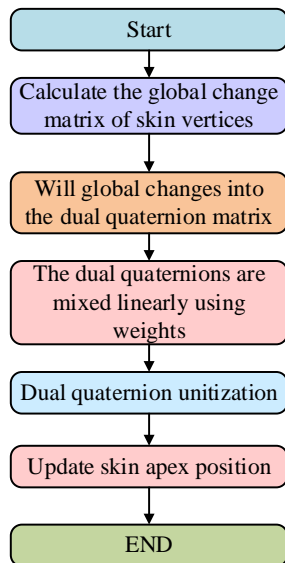


Fig. 6. Work flow of dual quaternion mixed skinned mesh algorithm.

#### IV. PERFORMANCE TESTING AND APPLICATION ANALYSIS OF COMPUTER SKELETAL SKINNED MESH ALGORITHM ANIMATION DESIGN

To verify the application effect of the bone SMA designed in the design of 3DVHMs, relevant performance tests and effect evaluation experiments were designed, and the results were analyzed and discussed.

##### A. Performance Testing of Weight Calculation Method Based on Posture Matching and Dual Quaternion Hybrid Skinned Mesh Algorithm

Experimental Environment Setting: The experiment was conducted on an operating system running on Windows 7, i7 CPU, GTX1060 GPU, and 16GB of memory. All algorithm models were implemented using C++ and Python programming. Firstly, the designed posture matching-based Extended Bounding Box (EBB) weight calculation method were compared with other weight calculation methods for skin vertices, including Heat Balance Principle Algorithm (HBPA), Approximation Calculation of Skeletal Projection (ACKP), and Hand brush weight (HBW). Weight smoothness and stability were selected as the evaluation indicators for testing. Fig. 7 shows the experimental results. The EBB-based weight calculation method, which corresponded to the pose of the sports skeleton and skin skeleton models, performed well in the smoothness of skin surface weight. After 180 iterations, its weight smoothness finally stabilized at 90.08%, which was significantly better than other methods and 20.05 percentage points higher than HBPA of 70.03%. Meanwhile, this method had better stability in weight calculation and lower error rates for different models.

To conduct performance testing on SMA, a program was written using C++ language in the VC++6.0 software to implement the required algorithms for testing. The designed Dual Quaternion Blending Skinning (DQBS) was compared with Spherical Hybrid Skinning Deformation Algorithm (SHSD), Skinning Algorithm Based on Position-Based Dynamics (SA-PBD), and traditional linear hybrid SMA. 1686 sets of 3D virtual character models created by the design and modeling team of a certain animation development company were selected as the test dataset, which was divided into a training set and a testing set in a 7:3 ratio.

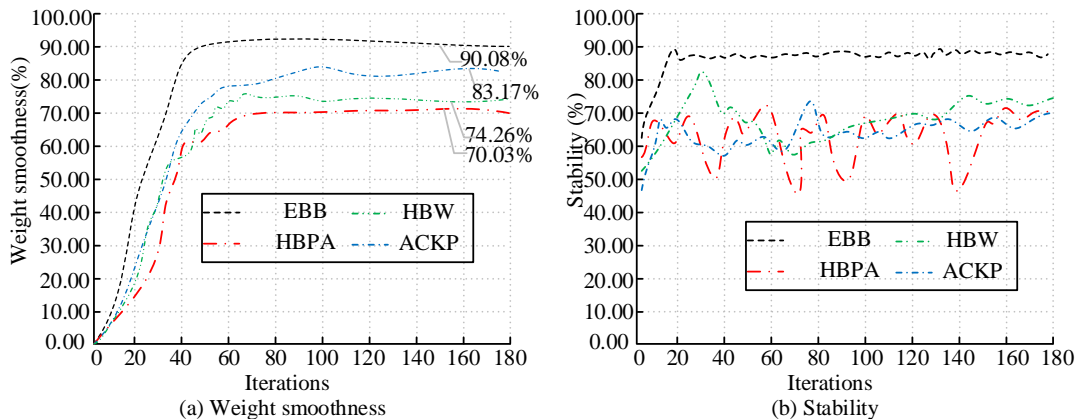


Fig. 7. Comparison of weight smoothness and stability of different weight calculation methods.

Comparing the precision and recall of four SMA algorithms, Fig. 8 shows the PR curves of different algorithms. PR is a curve drawn with precision as the vertical axis and recall as the horizontal axis. When the precision of the designed DQBS was 80% and 90%, the corresponding recall was 75.89% and 85.98%, respectively. In contrast, when the precision was 90, the recall of SHSD, SA-PBD, and LBS was 61.98%, 57.74%, and 50.16%, respectively. The precision and recall of SHSD, SA-PBD, and LBS were significantly lower than those of the study design method.

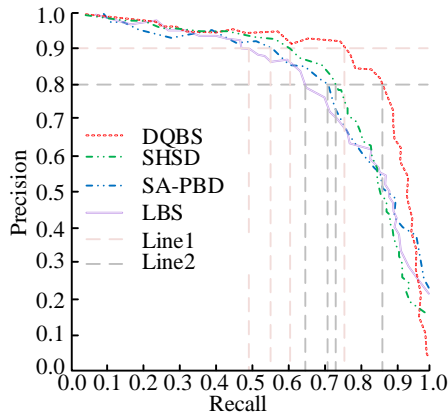


Fig. 8. Comparison of accuracy and recall rates of different skin algorithms.

The Receiver Operating Characteristic (ROC) curve is selected to evaluate different SMAs, and Fig. 9 shows the results. AUC is the area below ROC, used to measure the stability of model performance and overall effectiveness. Different SMAs had different AUC values, and the designed DQBS had the highest AUC, reaching 0.927. SA-PBD had the smallest AUC, only 0.634. Overall, the designed SMA performs better.

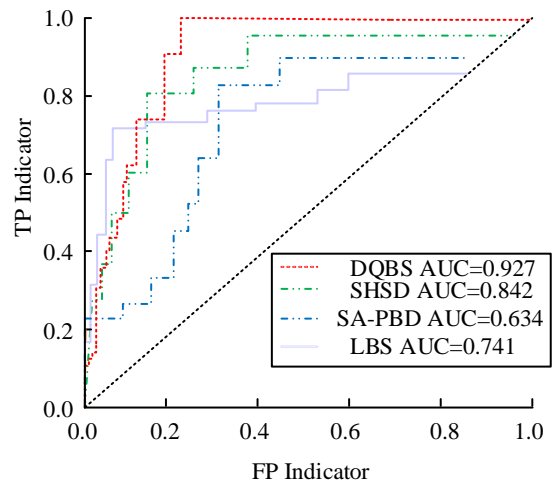


Fig. 9. Comparison of ROC curves for different skin algorithms.

**B. Evaluation of Skinned Effects for 3d Virtual Human Based on Dual Quaternion Hybrid Skin**

The simulation system for skin animation uses Visual Studio 2010 as the development platform and motion capture data ASF/AMC files designed and developed by Acclaim Games. The skin effects of SMA with inherent defects were compared, and the knee bone bending, armpit bending, and elbow bending with larger joint rotation were selected. From an objective evaluation perspective, smoothness and volume retention rate were selected as evaluation indicators for effect comparison. Fig. 10 shows the experimental results. After 50 iterations, the smoothness and volume retention of the SMA in three different parts were all above 90.00%. The designed model did not show obvious collapse, and the volume loss of the model was relatively small.

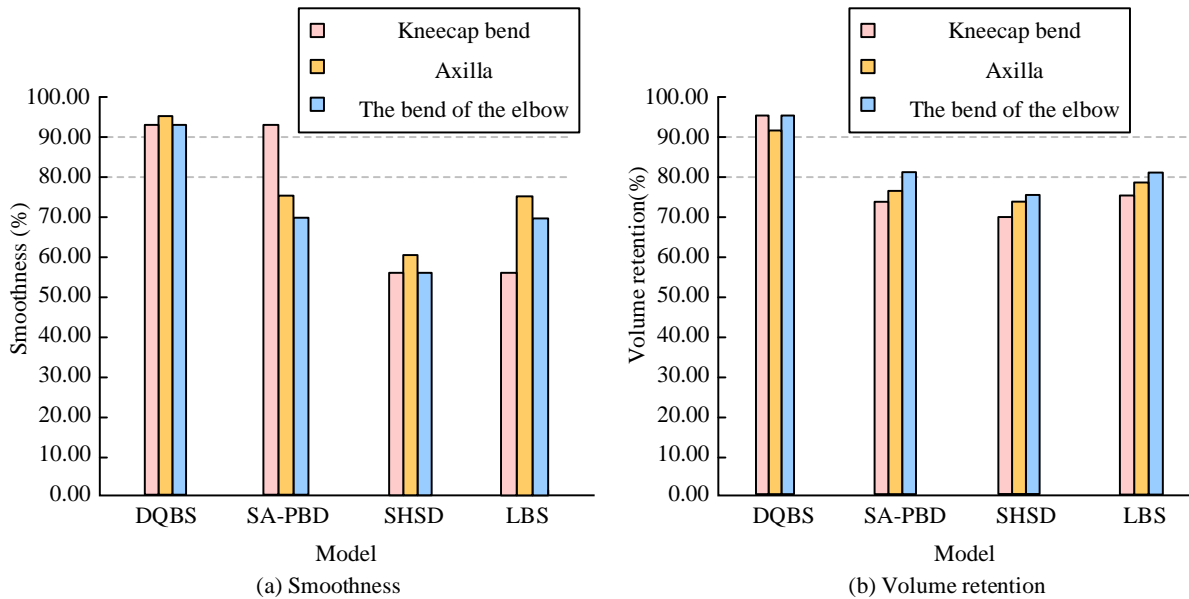


Fig. 10. Comparison of smoothness and volume retention of different skinning algorithms.



The study selected objective and subjective evaluation indicators, including model generation time, bone generation time, skin time, memory usage, stability, texture preservation ability, usability, and scalability. Table I shows the statistical results. The calculation time of DBQS was short, and the skinning time was only 0.49S. Its entire weight allocation, vertex transformation, and interpolation processes were calculated at a fast speed, and the memory usage was only 1247K, indicating good performance. In addition, the stability and texture retention ability of DBQS reached 90.63% and 80.68%, respectively, significantly higher than other SMAs. The subjective evaluation indicators had obvious advantages in usability and scalability, both exceeding 85%.

Finally, animation fluency and appearance realism were selected to rate the 3DVHM. A total of 30 users were gathered to evaluate the generation models of different SMAs from the perspectives of arms, legs, abdomen, and head. Fig. 11 shows the experimental results. Authenticity is the evaluation of whether the final effect of a model is realistic and whether it can provide users with an immersive feeling. Fluency is the evaluation of whether the animation effect is smooth and natural, especially in complex deformations and actions, whether it can maintain good continuity and fluency. In Fig. 11, the fluency and authenticity scores of DBQS were relatively high in different parts, with median scores ranging from 70 to 80. Its overall effect is good.

TABLE I. COMPARISON OF SUBJECTIVE AND OBJECTIVE EVALUATION OF DIFFERENT SKIN ALGORITHMS

Evaluating indicator	DBQS	SA-PBD	SHSD	LBS
Model generation time	13.35S	15.19S	12.73S	18.25S
Bone formation time	1.20S	1.32S	1.29S	1.41S
Skin time	0.49S	0.52S	0.74S	0.96S
Internal memory	1247K	2871K	3217K	4126K
Stability	90.63%	63.45%	73.01%	72.35%
Texture retention	80.68%	68.97%	76.17%	62.06%
Expandability	94.73%	72.01%	69.39%	84.14%
Ease of use	86.21%	74.58%	66.37%	77.69%

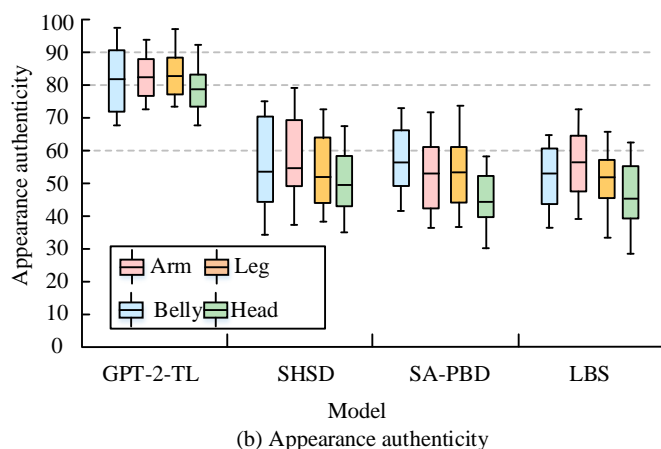
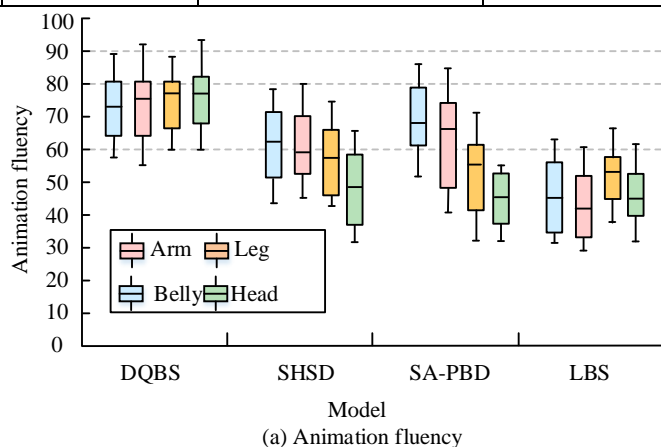


Fig. 11. Animation fluency and appearance authenticity scores of different skin algorithms.

## V. CONCLUSION

The 3D virtual human skeleton skin animation technology is the key to 3DVCA creation. To achieve more realistic 3D virtual human animation effects and achieve precise bone skin deformation, a skin vertex weight calculation and hybrid SMA for virtual characters were studied and designed. These experiments confirm that the designed EBB-based weight calculation algorithm performs well in weight smoothness and stability, with the highest smoothness reaching 90.08%, which is 20.05 percentage points higher than the lowest value. After 50 iterations, the designed SMA has higher smoothness and volume retention in different parts, and there is no obvious collapse phenomenon and the volume loss rate is relatively small. The calculation time of DBQS is short, the skinning time is only 0.49S, and the memory usage is only 1247K. Its stability and texture retention ability reaches 90.63% and 80.68%, respectively. Its subjective evaluation indicators have obvious advantages in usability and scalability. DBQS has high scores for fluency and authenticity in four different parts, with median scores ranging from 70 to 80. Its overall effect is more realistic. The designed SMA has obvious advantages in the application of 3D virtual human animation design. The skin of virtual characters can naturally follow the movement changes of bones during animation. This is a more realistic presentation of character animation, which is the technical key to improving animation realism, smoothness, and rendering efficiency. However, research has adopted a double-layer structure to model virtual humans, and future research can adopt more accurate skeleton extraction algorithms. The study did not involve changes in the muscles of the characters, nor did it simulate facial expressions and expressions, which can be a focus of future research work.

## VI. SYMBOL INDEX

All conforming explanations in the text are shown in Table II.

TABLE II. INTERPRETATION OF SYMBOLS USED IN THE STUDY

Notation	Interpretations
3DVCA	3D Virtual Character Animation
3DVHM	3D Virtual Human Model
SMA	Skinned Mesh Algorithm
EBB	Extended Bounding Box
HBPA	Heat Balance Principle Algorithm
HBW	Hand brush weight
DQBS	Dual Quaternion Blending Skinning
SA-PBD	Skinning Algorithm Based on Position-Based Dynamics
SHSD	Spherical Hybrid Skinning Deformation Algorithm
ROC	Receiver Operating Characteristic
LBS	Linear Blending Skinning

## REFERENCES

- [1] Demirel H O, Salman A, Vincent G D, Duffy. Digital human modeling: A review and reappraisal of origins, present, and expected future methods for representing humans computationally. *International Journal of Human-Computer Interaction*, 2022, 38(10): 897-937.
- [2] Yang Y. The skinning in character animation: A survey. *Academic Journal of Computing & Information Science*, 2022, 5(4): 4-17.
- [3] Zhang J. Survey of Skinning Method in 3D Character Animation. *Academic Journal of Computing & Information Science*, 2023, 6(9): 110-114.
- [4] Amin, S. N., Shivakumara, P., Jun, T. X., Chong, Y. K., Zan, D. L. L., Rahavendra, R. An Augmented Reality-Based Approach for Designing Interactive Food Menu of Restaurant Using Android. *Artificial Intelligence and Applications*. 2023, 1(1): 26-34.
- [5] Liu C, Wang A, Bu C, Wang W, Fang Z, He S. Reconstructing detailed human body using a viewpoint auto-changing RGB-D sensor for rescue operation. *IEEE Sensors Journal*, 2022, 22(13): 13262-13272.
- [6] Kruppa K, Kunkli R, Hoffmann M. A skinning technique for modeling artistic disk B-spline shapes. *Computers & Graphics*, 2023, 115(6): 96-106.
- [7] Wu Y, Umetani N. Two-Way Coupling of Skinning Transformations and Position Based Dynamics. *Proceedings of the ACM on Computer Graphics and Interactive Techniques*, 2023, 6(3): 1-18.
- [8] Hachette O, Canezin F, Vaillant R, Mellado N, Barthe L. Automatic shape adjustment at joints for the implicit skinning. *Computers & Graphics*, 2022, 102(1): 300-308.
- [9] Peng T, Kuang J, Liang J, Hu X, Miao J, Zhu P, Li L. GSNet: Generating 3D garment animation via graph skinning network. *Graphical Models*, 2023, 129(5): 101197-101206.
- [10] Mouhou A A, Saaidi A, Yakhlef M B, Abbad K. Virtual hand skinning using volumetric shape. *International Journal of Computer Aided Engineering and Technology*, 2023, 18(3): 77-96.
- [11] Zhao R, Mi J, Jiang Y, Chen Z, Wang H. 4DFA: Four-Dimensional Full-Anatomy Reconstruction of Individualized Digital Human Models Based on Motion Videos. *Advances in Engineering Technology Research*, 2023, 4(1): 269-269.
- [12] Singla K, Nand P. Reconstructing dynamic human shapes from sparse silhouettes via latent space optimization of Parametric shape models. *Turkish Journal of Electrical Engineering and Computer Sciences*, 2023, 31(2): 295-311.
- [13] Chen X, Jiang T, Song J, Rietmann M, Geiger A, Black M J, Hilliges O. Fast-SNARF: A fast deformer for articulated neural fields. *IEEE Transactions on Pattern Analysis and Machine Intelligence*, 2023, 45(10): 11796 – 11809.
- [14] Li Y D, Tang M, Chen X R. D-Cloth: Skinning-based Cloth Dynamic Prediction with a Three-stage Network. *COMPUTER GRAPHICS forum*. 2023, 42(7): 14937-14939.
- [15] Santesteban I, Otaduy M, Thuerey N, Casas D, Ulfner. Untangled layered neural fields for mix-and-match virtual try-on. *Advances in Neural Information Processing Systems*, 2022, 35(5): 12110-12125.
- [16] Wu Y, Chen Z, Liu S, Ren Z, Wang S. Casa: Category-agnostic skeletal animal reconstruction. *Advances in Neural Information Processing Systems*, 2022, 35(7): 28559-28574.
- [17] Lu Y, Yu H, Ni W, Song L. 3D real-time human reconstruction with a single RGBD camera. *Applied Intelligence*, 2023, 53(8): 8735-8745.
- [18] Zheng Z, Yu T, Liu Y, Dai Q. Pamir: Parametric model-conditioned implicit representation for image-based human reconstruction. *IEEE transactions on pattern analysis and machine intelligence*, 2021, 44(6): 3170-3184.
- [19] Chandran P, Zoss G, Gross M, Gotardo P, Bradley D. Shape Transformers: Topology-Independent 3D Shape Models Using Transformers. *Computer Graphics Forum*. 2022, 41(2): 195-207.
- [20] Pham J, Wyetzner S, Pfaller M R, Parker D W, James D L, Marsden A L. svMorph: Interactive geometry-editing tools for virtual patient-specific vascular anatomies. *Journal of Biomechanical Engineering*, 2023, 145(3): 31001-31008.